Modelling cosmic rays and gamma rays in the Galaxy

Andrew W. Strong* and Igor V. Moskalenko*†

*Max-Planck-Institut für extraterrestrische Physik, D-85740 Garching, Germany
†Institute for Nuclear Physics, Moscow State University, 119 899 Moscow, Russia

Abstract. An extensive program for the calculation of galactic cosmic-ray propagation has been developed. This is a continuation of the work described in [1]. The main motivation for developing this code [2] is the prediction of diffuse Galactic gamma rays for comparison with data from the CGRO instruments EGRET, COMPTEL, and OSSE. The basic spatial propagation mechanisms are (momentum-dependent) diffusion, convection, while in momentum space energy loss and diffusive reacceleration are treated. Primary and secondary nucleons, primary and secondary electrons, and secondary positrons are included. Fragmentation and energy losses are computed using realistic distributions for the interstellar gas and radiation fields.

INTRODUCTION

We are developing a model which aims to reproduce self-consistently observational data of many kinds related to cosmic-ray origin and propagation: direct measurements of nuclei, electrons and positrons, gamma rays, and synchrotron radiation. These data provide many independent constraints on any model and our approach is able to take advantage of this since it must be consistent with all types of observation. We emphasize also the use of realistic astrophysical input (e.g., for the gas distribution) as well as theoretical developments (e.g., reacceleration). The code is sufficiently general that new physical effects can be introduced as required. The basic procedure is first to obtain a set of propagation parameters which reproduce the cosmic ray B/C ratio, and the spectrum of secondary positrons; the same propagation conditions are then applied to primary electrons. Gamma-ray and synchrotron emission are then evaluated. Models both with and without reacceleration are considered. The models are three dimensional with cylindrical symmetry in the Galaxy, the basic coordinates being (R, z, p) where R is Galactocentric radius, z is the distance from the Galactic plane and p is the total particle momentum. The numerical solution of the transport equation is based on a

Crank-Nicholson implicit second-order scheme. In the models the propagation region is bounded by $z = z_h$ beyond which free escape is assumed. A value $z_h = 3$ kpc has been adopted since this is within the range which is consistent with studies of ^{10}Be/Be and synchrotron radiation. For a given z_h the diffusion coefficient as a function of momentum is determined by B/C for the case of no reacceleration; with reacceleration on the other hand it is the reacceleration strength (related to the Alfvén speed v_A) which is determined by B/C. Reacceleration provides a natural mechanism to reproduce the B/C ratio without an ad-hoc form for the diffusion coefficient [3,4]. The spatial diffusion coefficient for the case *without* reacceleration is $D = \beta D_0$ below rigidity ρ_0, $\beta D_0(\rho/\rho_0)^\delta$ above rigidity ρ_0, where β is the particle speed. The spatial diffusion coefficient *with* reacceleration assumes a Kolmogorov spectrum of weak MHD turbulence so $D = \beta D_0(\rho/\rho_0)^\delta$ with $\delta = 1/3$ for all rigidities. For this case the momentum-space diffusion coefficient is related to the spatial one [4]. The injection spectrum of nucleons is assumed to be a power law in momentum. The interstellar hydrogen distribution uses HI and CO surveys and information on the ionized component; the Helium fraction of the gas is taken as 0.11 by number. The interstellar radiation field for inverse Compton losses is based on stellar population models and IRAS and COBE data, plus the cosmic microwave background. Energy losses for electrons by ionization, Coulomb, bremsstrahlung, inverse Compton and synchrotron are included, and for nucleons by ionization and Coulomb interactions. The distribution of cosmic-ray sources is chosen to reproduce the cosmic-ray distribution determined by analysis of EGRET gamma-ray data [5]. The bremsstrahlung and inverse Compton gamma rays are computed self-consistently from the gas and radiation fields used for the propagation. The π^0-decay gamma rays are calculated explicitly from the proton and Helium spectra using [6]. The secondary nucleon and secondary $e^\pm$ source functions are computed from the propagated primary distribution and the gas distribution, and the anisotropic distributions of $e^\pm$ in the $\mu^\pm$ system was taken into account [7].

ILLUSTRATIVE RESULTS

Some results obtained are shown in the Figures. The energy dependence of the B/C ratio, and local *proton and Helium spectra* are shown in Figs. 1 and 2. The spectrum of *primary electrons* is shown in Fig. 6. The adopted electron injection spectrum has a power law index –2.1 up to 10 GeV; this is chosen using the constraints from synchrotron and from gamma rays. The electron spectrum is consistent with the direct measurements around 10 GeV where solar modulation is small and it also satisfies the constraints from $\frac{e^+}{e^- + e^+}$. Above 10 GeV a break is required in the injection spectrum to at least –2.4 for agreement with direct measurements (which may however not be necessary if local sources dominate the directly measured high-energy electron spectrum).

The synchrotron spectrum at high Galactic latitudes (Fig. 3) is important since its shape constrains the shape of the 1–10 GeV electron spectrum. An injection index –2.1 (without reacceleration) is the steepest which is allowed by the radio data over the range 38 to 1420 MHz. As illustrated, an index –2.4 as often used (e.g., [8]) gives a synchrotron spectrum which is too steep.

The modelled *gamma-ray* spectrum for the inner Galaxy, shown here for the case of no reacceleration (Fig. 4), fits well the COMPTEL [9] and EGRET [5] data between 1 MeV and 1 GeV beyond which there is the well-known excess not accounted for by π^0-decay with the standard nucleon spectrum [10,11]. The electron spectrum used here is increased by a factor 2 over that shown in Fig. 6; this is required to reproduce well the observed gamma intensities. It is still within the range allowed by the positron fraction (see below), and the shape accords well with the flatter electron injection spectrum required by synchrotron data (Fig. 3). Inverse Compton is dominant below 10 MeV, bremsstrahlung becomes important for 3–200 MeV. The lower bremsstrahlung combined with π^0-decay leads to a good fit to the flat spectrum observed in this range, in contrast to previous attempts to model the spectrum with a steeper bremsstrahlung spectrum [8]. The 10–30 MeV γ-ray longitude profile (Fig. 5) at low latitudes from this model can be compared with that from COMPTEL [9]. The e^+ *spectrum* (Fig. 6) and the *positron fraction* (Fig. 7) agree well with the most recent data compilation for 0.1–10 GeV [7].

This study indicates that it is possible to construct a model satisfying a wide range of observational constraints and provides a basis for future developments.

More details can be found on *http://www.gamma.mpe–garching.mpg.de/~aws/aws.html*

REFERENCES

1. Strong A.W., Youssefi G., *Proc. 24th ICRC* **3**, 48 (1995)
2. Strong A.W., Moskalenko I.V., Schönfelder V., *Proc. 25th ICRC*, OG 8.1.1 (1997)
3. Heinbach U., Simon M., *ApJ* **441**, 209 (1995)
4. Seo E.S., Ptuskin V.S., *ApJ* **431**, 705 (1994)
5. Strong A.W., Mattox J.R., *A&A* **308**, L21 (1996)
6. Dermer C.D., *A&A* **157**, 223 (1986)
7. Moskalenko I.V., Strong A.W., *ApJ*, submitted (1997)
8. Strong A.W. et al., *A&AS* **120**, C381 (1996)
9. Strong A.W., et al., in *AIP Proc.*, 1997, this Symposium
10. Hunter S.D., et al., *ApJ* **481**, 205 (1997)
11. Mori M., *ApJ* **478**, 225 (1997)
12. Webber W.R., et al., *ApJ* **457**, 435 (1996)
13. Seo E.S., et al., *ApJ* **378**, 763 (1991)
14. Engelmann J.J., et al., *A&A* **233**, 96 (1990)
15. Protheroe R.J., *ApJ* **254**, 391 (1982)
16. Barwick S.W., et al., *ApJL* **482**, L191 (1997)

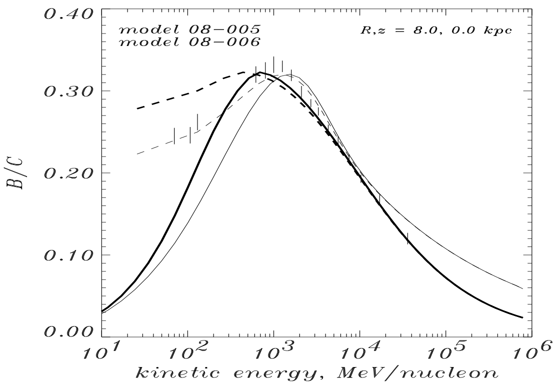

FIGURE 1. The energy dependence of the B/C ratio can be reproduced with $D_0 = 2.0\times10^{28}$ cm^{2}s^{-1}, $\delta = 0.6$, $\rho_0 = 3$ GV/c without reacceleration (thick line) and $D_0 = 4.2\times10^{28}$ cm^{2}s^{-1}, $v_A = 20$ km s^{-1} with reacceleration (thin line). Dashed lines are modulated to 500 MV. Data from [12].

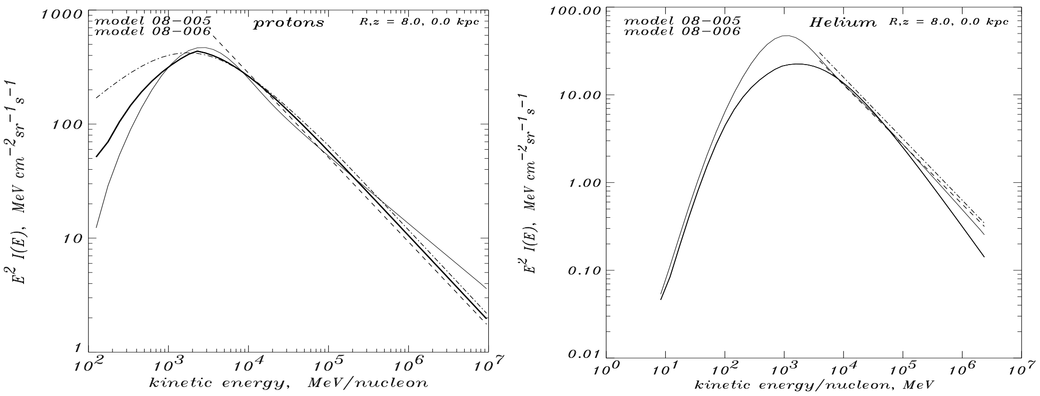

FIGURE 2. *Left panel:* the local proton spectrum for injection index 2.15 (thin solid line), 2.25 (thick solid line) without and with reacceleration respectively, compared with the measured 'interstellar' spectrum (dashed [13] and dashed-dot [11] lines). *Right panel:* the Helium spectrum with injection index 2.25 (thin solid line), 2.45 (thick solid line) without and with reacceleration respectively, compared with the measured 'interstellar' spectrum (dashed [13] and dashed-dot [14] lines).

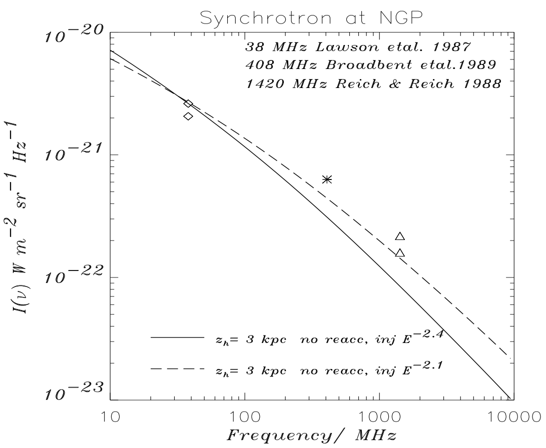

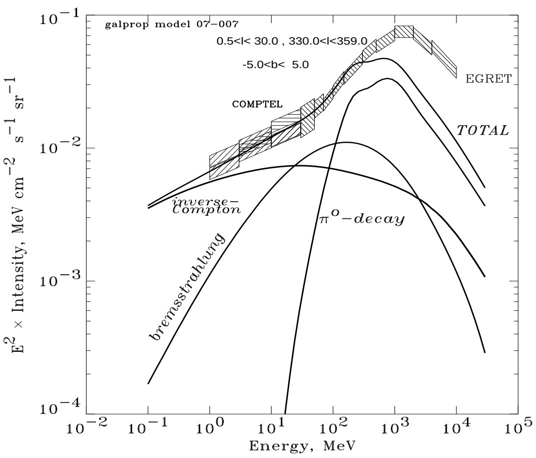

FIGURE 3. The synchrotron spectrum at the NGP, and predictions for electron injection indices –2.1 (dashed line) and –2.4 (solid line).

FIGURE 4. The γ-ray spectrum for the inner Galaxy, $330° < l < 30°, |b| < 5°$. EGRET data [5], COMPTEL data [9].

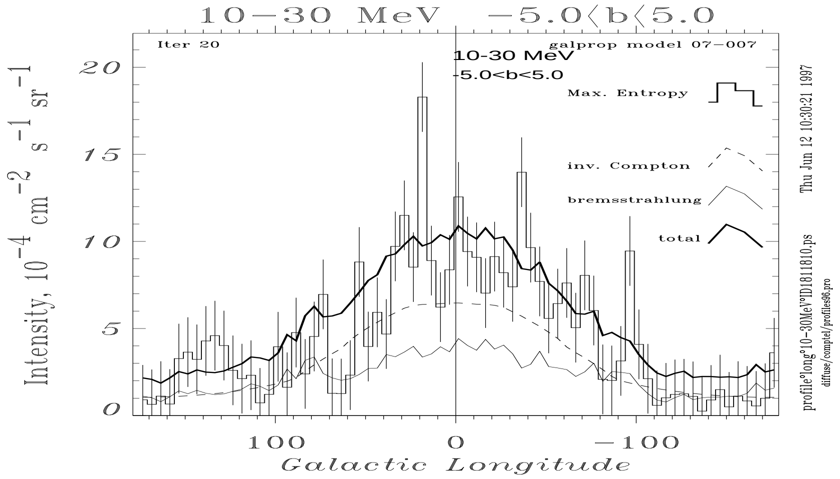

FIGURE 5. Longitude distribution of gamma rays in energy range 10-30 MeV. Histogram: COMPTEL [9], dashed: inverse Compton, thin line: bremsstrahlung, thick line: total.

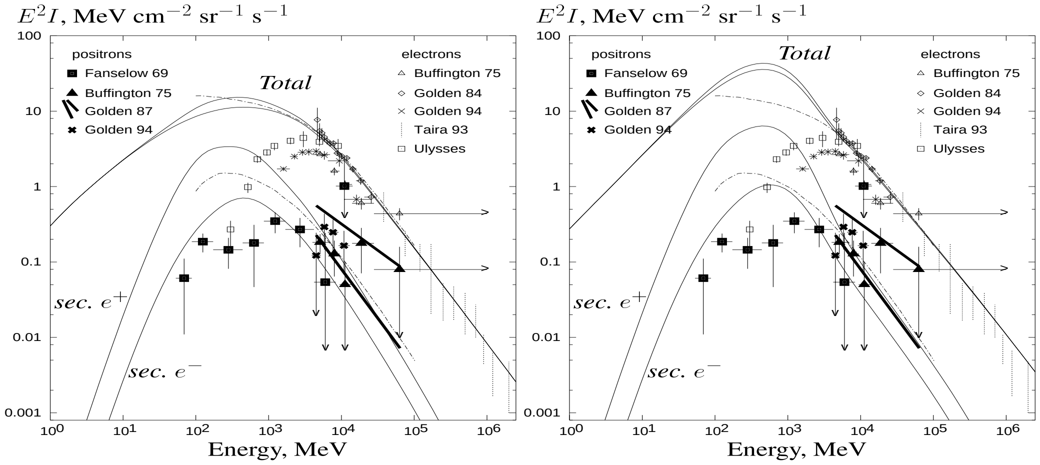

FIGURE 6. Spectra of secondary $e^{\pm}$, and of primary electrons. Full lines: our model with no reacceleration (left) and with reacceleration (right). Dash-dotted lines by Protheroe [15]: lower is his leaky-box prediction for e^+, upper is his adopted electron spectrum.

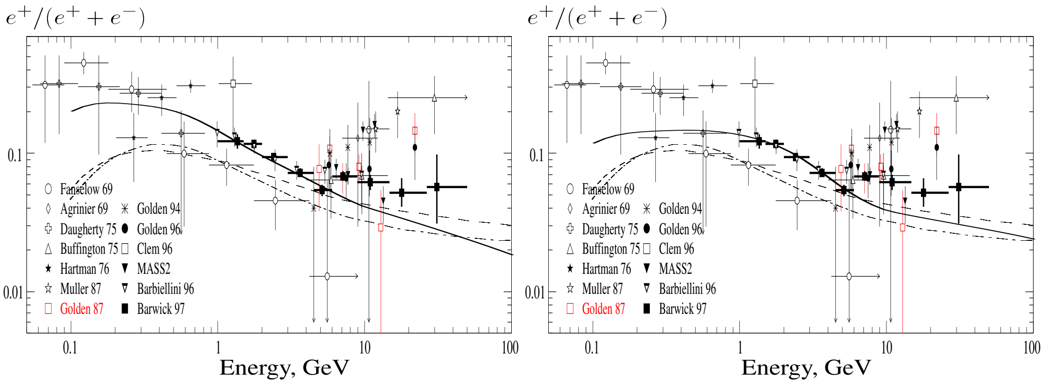

FIGURE 7. Positron fraction for model with no reacceleration (left panel) and with reacceleration (right panel). Dashed and dash-dotted lines by Protheroe [15]: his predictions of the leaky-box and diffusive halo models respectively. The data collection is taken from [16].